



Structural Delineation and Identification of Mineralisation Zones Using Aeromagnetic Data in Katsina State, Northwestern Nigeria.



Galadima, Hadi Buhari^{1*}, Akpaneno, Aniefiok Francis², & Abubakar Sada³

^{1,2,3}Department of Physics Federal University Dutsinma, Katsina State, Nigeria

Corresponding Author's Email: slimexcom@gmail.com

*Corresponding Author Email: slimexcom@gmail.com

ABSTRACT

Eight High-resolution aeromagnetic data (HRAM) were used to delineate subsurface structures and identify potential mineralisation zones in parts of Katsina State, northwestern Nigeria, the data sets are specifically Sheet 33 (Ruma), Sheet 34 (Katsina), Sheet 55 (Dutsin Ma), Sheet 65 (Musawa), Sheet 78 (Funtua), Sheet 79 (Malumfashi), Sheet 101 (Maska) and Sheet 102 (Zaria). Four edge-detection techniques including Analytic Signal (AS), First Vertical Derivative (FVD), Second Vertical Derivative (SVD), and Horizontal Gradient Magnitude (HGM) alongside the Centre for Exploration Targeting (CET) plug-in, were applied to map lineaments such as faults, dykes, and folds. The Total Magnetic Intensity (TMI) map revealed significant variations (32,933.563-33,079.871 nT), with high magnetic anomalies associated to ferromagnetic rich lithologies, including porphyritic granite and hypersthene quartz diorite. Structural trend analysis using rose diagrams revealed dominant WNW-ESE and NE-SW orientations, consistent with regional Pan-African tectonics. High AS amplitudes (0.091-0.259 nT/m) and high structural density zones correlate with potential mineralisation zones, particularly in the southeastern (Mai-Jiriya, Gwarzo) and northwestern (Charanchi, Mani) regions. A prominent NW-SE trending dyke-like feature through Mahazu and Ungwan Gagarau was identified as a structurally controlled mineralised corridor. Overlaying structural maps with geological data confirmed mineralisation within pelitic/muscovite schist and porphyritic granite, likely driven by magmatic intrusions. These findings demonstrate the efficacy of aeromagnetic surveys in mapping structural controls on mineralisation, providing a framework for targeted exploration in Nigeria's Schist Belt. Ground geophysical surveys and geochemical assays are recommended to validate these zones and assess economic potential.

Keywords:

Aeromagnetic survey,
Structural delineation,
Mineralisation zones,
Katsina State,
Edge detection,
Analytic signal.

INTRODUCTION

Magnetic surveys are conducted by measuring the strength and direction of the Earth's magnetic field at various surface points to detect subsurface structures, faults, and mineral deposits (Encyclopedia of Geophysics, 2012). The study of Earth's magnetism and behavior is the oldest branch of geophysics (Elawadi *et al.*, 2004; Telford *et al.*, 1990). Most mineral deposits are hidden underground, and their detection relies on physical properties that distinguish them from surrounding materials. The growing global demand for metals and the significant rise in oil and gas use over the past fifty years have driven the development of geophysical methods with enhanced sensitivity for identifying hidden deposits and structures (Zlotnikov, 2012; Salawu *et al.*, 2023).

Techniques such as seismic, gravity, electrical resistivity, induced polarization, self-potential, electromagnetic, radar, and magnetic methods are selected based on the target deposit's responsive properties (Kearey *et al.*, 2002).

Aeromagnetic surveys have become one of the most important tools in geophysical exploration, mapping subsurface geological structures and mineralization zones by detecting variations in the Earth's magnetic field (Kearey *et al.*, 2002; Reynolds, 2011). In mineral rich areas like Nigeria's Schist Belt, these surveys are valuable for identifying faults, dykes, and folds that control ore deposits such as gold, copper, and iron ore (Ajibade *et al.*, 1987; Airo, 2007; Andongma *et al.*, 2021). Aeromagnetic data are particularly effective in gold exploration due to

their ability to detect hydrothermal alteration zones and associated magnetic mineral depletion (Airo, 2007). Aeromagnetic surveys offer advantages like rapid data collection, extensive area coverage per time unit, and the ability to overcome challenges faced in ground-based magnetic prospecting. Magnetic methods explore geological variations caused by differences in the geomagnetic field, which stem from the magnetic properties of subsurface rocks (Ge *et al.*, 2020; Olasunkanmi *et al.*, 2020; Kearey *et al.*, 2002; Ekwok *et al.*, 2021). Aeromagnetic surveys, a widely used airborne geophysical technique, are recognized as a primary tool for mapping highly magnetized materials (Murthy, 2007). Magnetite is the most prevalent magnetic mineral globally, with other magnetic minerals being less significant (Grant, 1985). Aeromagnetic surveys map magnetite in rocks beneath the aircraft are often used as reconnaissance tools, though their value for evaluating potential sites is increasingly recognized due to their unique data outlined their roles as:

- Identifying recent lithologies in heavily metamorphosed terrains or under sand/recent cover where they are otherwise undetectable.
- Detecting and interpreting faulting, shearing, and fracturing as potential hosts for minerals or indicators of epigenetic stress-related mineralization in nearby rocks.
- Identifying and defining post-tectonic intrusions, such as zoned syenite or carbonatite complexes, kimberlites, tin-bearing granites, and mafic intrusions.
- direct discovery of certain iron ore deposits (Usman *et al.*, 2025). Aeromagnetic surveys are frequently employed as reconnaissance instruments, but because of the distinctive

information they offer, there has been a growing acknowledgement of their utility for assessing potential sites.

Katsina State, located in northwestern Nigeria, lies within this belt, characterized by Precambrian basement rocks and minor sedimentary cover (Kogbe, 1976; Oyeniyi *et al.*, 2022). Despite its mineral potential, detailed structural mapping in this region remains limited, hindering exploration efforts. The significance lies in providing a cost-effective framework for mineral exploration, supporting Nigeria's economic diversification through solid mineral development (Lawal *et al.*, 2024). By integrating multiple edge-detection methods and geological overlays, this study enhances the understanding of structural controls on mineralisation, offering a foundation for targeted fieldwork and resource assessment.

The aim of the study is to assess the structural delineation and identification of mineralisation zones using aeromagnetic data in Katsina State.

The objectives are to; apply Analytic Signal (AS), First Vertical Derivative (FVD), Second Vertical Derivative (SVD), and Horizontal Gradient Magnitude (HGM) techniques to map lineaments; use the CET plug-in for complex structural analysis; correlate high magnetic anomalies with structural density; and identify potential mineralisation zones.

Location, Extent and Elevation of the Study Area

The study area is primarily located in Katsina State (Figure 1), covering a land area of about 24,000 km². It is situated between longitudes 7° E and 8° E and latitudes 11° N and 13° N. Figure 2 displays the digital elevation model (DEM) illustrating the topographic variation of the area. The elevation ranges from a low of 413m around Wauni, Ruma, and Gidan Baure to 806m above sea level around Danja, Funtua, and Mai-Rijiyi

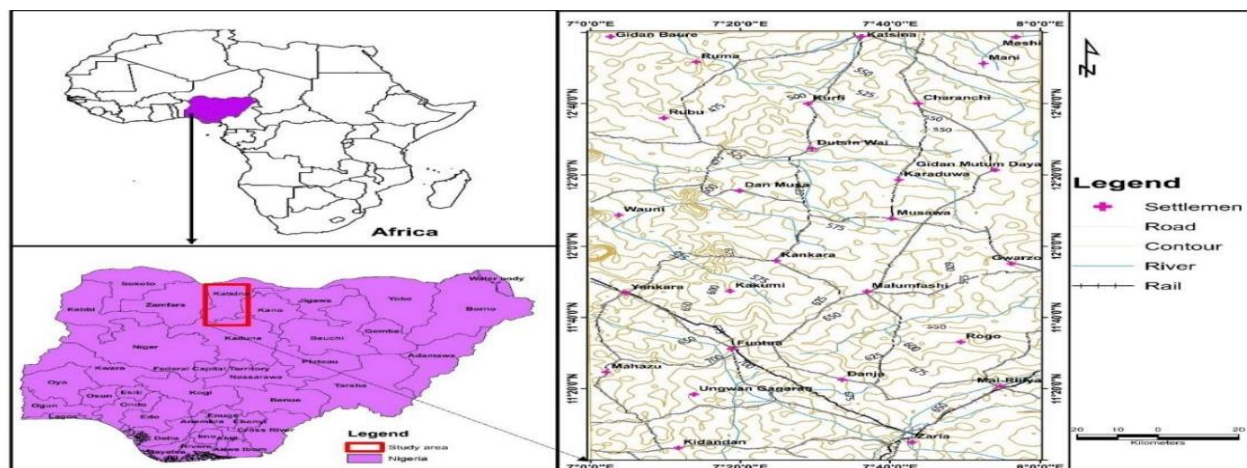


Figure 1 Showing Location of the Study Area (modified from NGS 2006)

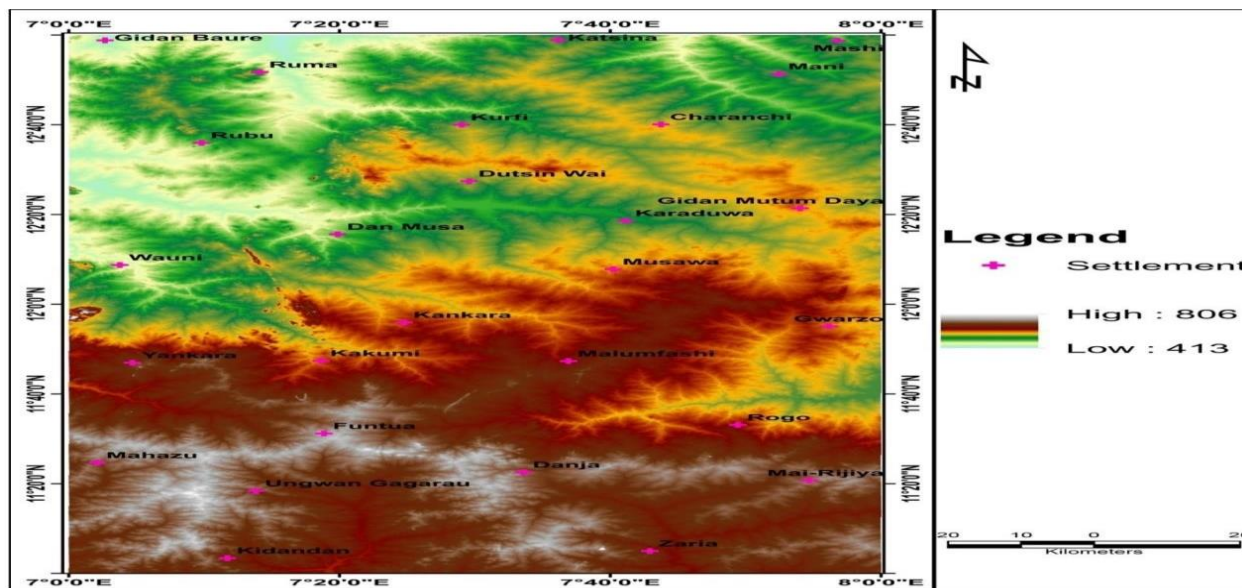


Figure 2 Digital Elevation Map (modified from NGS 2006)

Geology of the Study Area

The study area lies within the Nigerian Basement Complex, which form part of the Pan-African mobile zone situated between the West African and Gabon-Congo Cratons (Ferre *et al.*, 1998; Nzekwu and Abraham-Emmanuel, 2022). The region is dominated by Precambrian basement rocks, including gneisses, migmatites, and schists, with minor Cretaceous to Tertiary sediments of the Sokoto Basin (Kogbe, 1976). The Malumfashi Schist Belt, a key feature, contains metamorphosed sediments and volcanics, including pelitic/muscovite schist, porphyritic granite, and hypersthene quartz diorite (Ajibade *et al.*, 1988; Andongma *et al.*, 2021). These lithologies host minerals

such as gold, copper, and iron ore, often associated with structural features like the Katsina Fault and folds (Fitches *et al.*, 1985). The Pan-African orogeny around 650 million year ago shaped the region through highgrade metamorphism, faulting, and granite plutonism, creating structural pathway for mineralising fluids (Ibrahim, 2003; Salawu *et al.*, 2023). The study area’s topography varies from 413 m (Waini, Ruma) to 806 m (Danja, Funtua), influencing magnetic anomaly patterns due to lithological contrasts and structural deformation (NGSA, 2006). This complex geological setting makes aeromagnetic surveys ideal for mapping subsurface structures and identifying mineralisation zones.

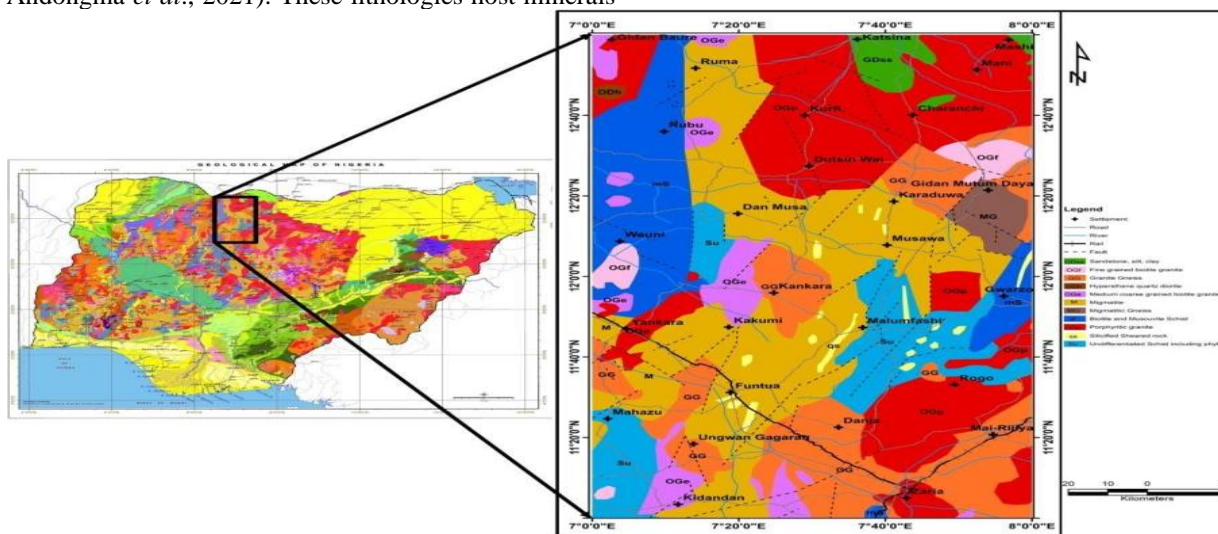


Figure 3 Showing the Geology of the Area (modified from NGS 2006)

MATERIALS AND METHODS

The materials used for this research are: Eight high resolution Aeromagnetic data sets (HRAM), specifically Sheet 33 (Ruma), Sheet 34 (Katsina), Sheet 55 (Dutsin Ma), Sheet 65 (Musawa), Sheet 78 (Funtua), Sheet 79 (Malumfashi), Sheet101 (Maska) and Sheet 102 (Zaria); Oasis Montaj v. 8.4.4 used for geological data processing and analysis to be able to enhance processing speed and efficiency of the large datasets; ArcGIS version 10.7.1 used to create, analyze, manage, and visualize spatial data; Surfer version 15 used to create and analyse the 3D surface models and contour maps, convert irregularly spaced data into regular grids using various interpolation. The methods used include:

Regional and Residual Separation

A composite magnetic map reveals two primary types of anomalies, varying from small to large in magnitude and typically overlapping. Large scale anomalies, known as regional patterns manifest as trends extending over broad areas with minimal variation, originating from deeper heterogeneities in the Earth's crust. Superimposed on these are smaller, localized anomalies termed residual anomalies which, though secondary in scale, are significant and often masked by regional fields. These residual anomalies may provide evidence of mineral ore bodies or reservoir-like structures.

Reduction to Pole

The reduction-to-pole (RTP) process transforms magnetic data to simulate a vertical magnetic field by removing dependency on the angle of magnetic inclination. This is achieved by convolving the magnetic field with a filter combining polarization and field-orientation factors (Spector *et al.*, 1970; Abraham-Emmanuel *et al.*, 2021). The RTP creates symmetrical anomalies over vertically dipping, non-remanent bodies, aiding interpretation under specific conditions. At low latitudes, an amplitude correction is required to prevent north-south signals from dominating. The RTP is expressed as:

$$L(\theta) = \frac{1}{[\sin(I_a) + i \cos(I) \cdot \cos(D - \theta)]} \quad (1)$$

Where:

I = geomagnetic inclination

I_a = inclination for amplitude correction

D = geomagnetic declination.

For two-dimensional structures, the anomaly peak correlates very closely with the analytical signal peak, indicating that the effect of remanent magnetism is relatively small.

Analytic Signal (AS)

The Analytic Signal (AS) method is vital for delineating boundaries of high and low magnetic features near the magnetic equator (Ansari and Alamdar, 2009). It centers anomaly peaks over their causative sources in both high- and low-latitude regions, is unaffected by magnetization direction, and is minimally impacted by noise (Macleod *et al.*, 1993; Salawu *et al.*, 2023). The AS is defined as the square root of the sum of the squares of a magnetic field's vertical and horizontal derivatives, as shown in:

$$|A(X, Y)| = \sqrt{\left(\frac{\partial T}{\partial x}\right)^2 + \left(\frac{\partial T}{\partial y}\right)^2 + \left(\frac{\partial T}{\partial z}\right)^2} \quad (2)$$

where $A(x,y)$ is the analytic signal amplitude at (x,y) , and T is the observable magnetic anomaly. This technique enables depth estimation of magnetic sources in the study area.

Derivatives

Derivatives enhance anomaly edges and shallow features, making them more sensitive to local effects than broader regional influences, thus providing sharper images than total field intensity maps. Small anomalies become more apparent amidst long-term regional variations. First derivatives (horizontal and vertical) clarify high-frequency features obscured by large-amplitude, low-frequency anomalies. The derivative is expressed as:

$$L(r) = r^n \quad (3)$$

where n = order of differentiation. The most common derivative maps are the first and second vertical derivatives (FVD and SVD).

The FVD enhances high-frequency patterns masked by large-amplitude, low-frequency anomalies. The SVD amplifies near-surface effects at the expense of deeper anomalies, measuring curvature where large curvatures indicate shallow anomalies. SVD is calculated from differences between closely spaced first derivatives, highlighting small anomalies and minimizing regional patterns. It is used to define body edges and enhance fault trends.

Mathematically, vertical derivatives measure potential field curvature, with zero SVD contours marking causal body edges. Zero magnetic contours of SVD often align with lithologic boundaries, while positive and negative anomalies correspond to surface exposures of mafic and felsic rocks, respectively.

Horizontal Gradient Magnitude (HGM): Detects magnetic contacts with reduced sensitivity to noise (Phillips, 2000; Lawal *et al.*, 2024).

CET Analysis: The CET plug-in in Oasis Montaj automated structural mapping, identifying lineaments from RTE data (Tawey *et al.*, 2023; Usman *et al.*, 2025). This approach is consistent with recent application of

CET grid analysis combined with edge detection techniques for structural mapping in the Nigerian Basement Complex (Tawey *et al.*, 2024)

Structural Trend Analysis: Structural Trend Analysis: Rose diagrams were used to evaluate dominant lineament orientations (Onyewuchi *et al.*, 2012; Ekwok *et al.*, 2021).

Mineralisation Zone Identification: High AS amplitudes were correlated with structural density and geological maps to pinpoint prospective zones.

RESULTS AND DISCUSSION

The Total Magnetic Intensity (TMI) map (Figure 4) shows magnetic intensity variations ranging from 32,933.563 nT to 33,079.871 nT. High magnetic anomalies are prominent in the northern (Katsina, Mani, Kurfi, Charanchi) and southeastern (Rogo, Mai-Jiriya) regions, while low anomalies dominate the central parts (Kankara, Malumfashi, Funtua).

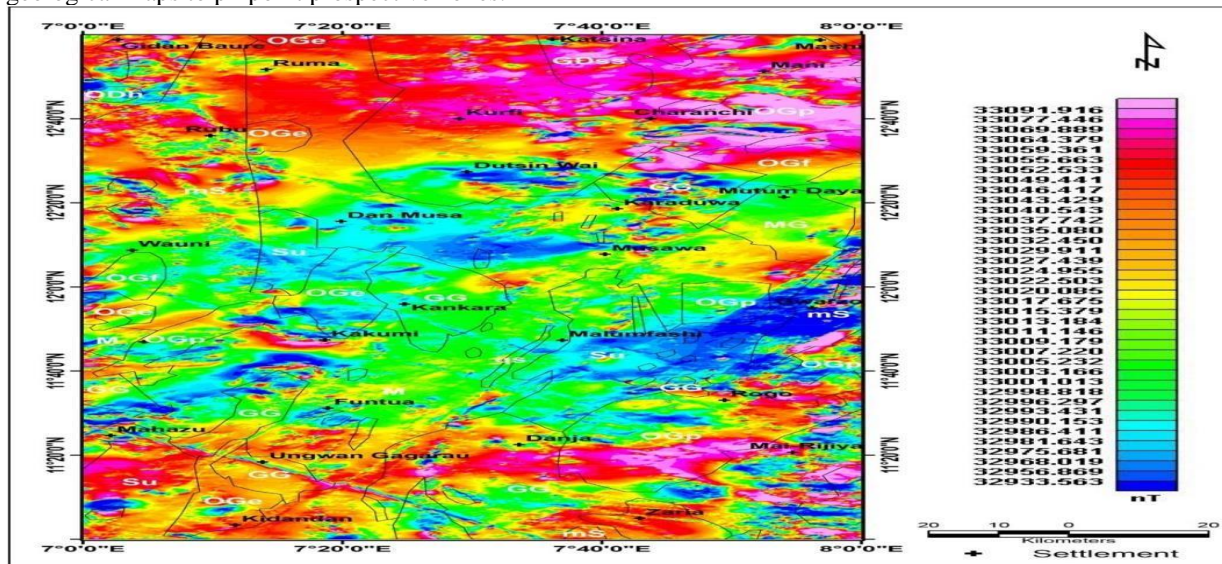


Figure 4: TMI map of the Area with the Geology. The Reduction to Equator (RTE) map (Figure 5) improves anomaly centering, with values highlighting better alignment of magnetic features (figure 6).

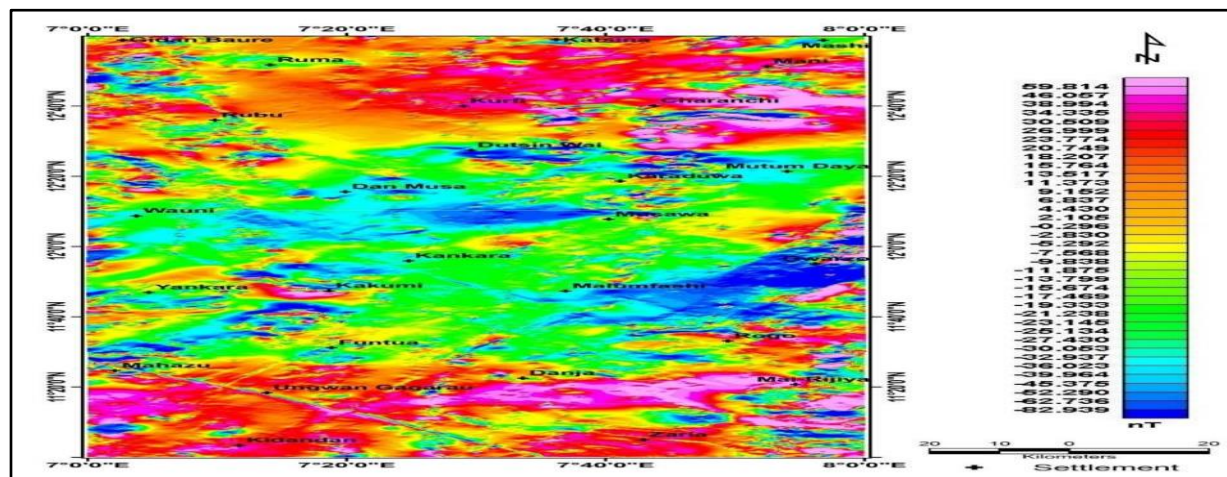


Figure 5: Residual Magnetic Intensity Reduced to Equator (TRE) Map

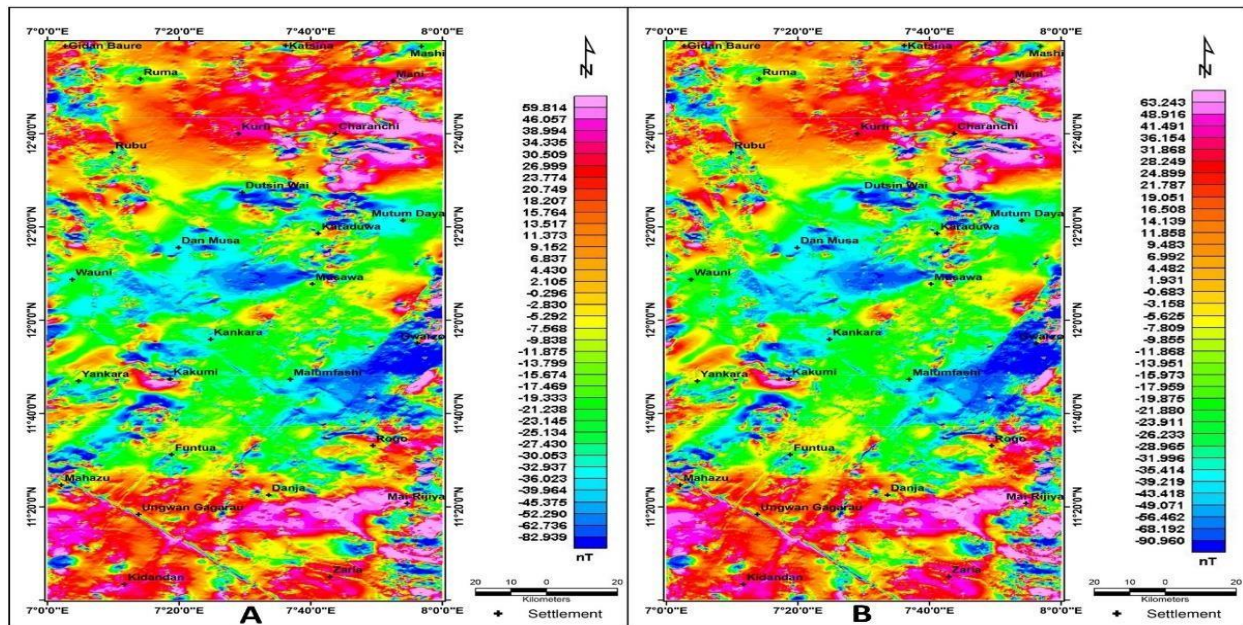


Figure 6: a. RTE map b. RMI map of the study area

The Analytic Signal (AS) map (Figure 7) reveals amplitudes ranging from 0.003 to 0.259 nT/m. These were classified into low (0.003–0.034 nT/m), medium (0.034–0.091 nT/m), and high (0.091–0.259 nT/m) amplitude zones. High AS amplitude zones are prominent

in the southeast (Mai-Jiriya, Gwarzo) and northwest (Charanchi, Mani). A prominent NW-SE trending dyke-like feature is visible through Mahazu and Ungwan Gagarau.

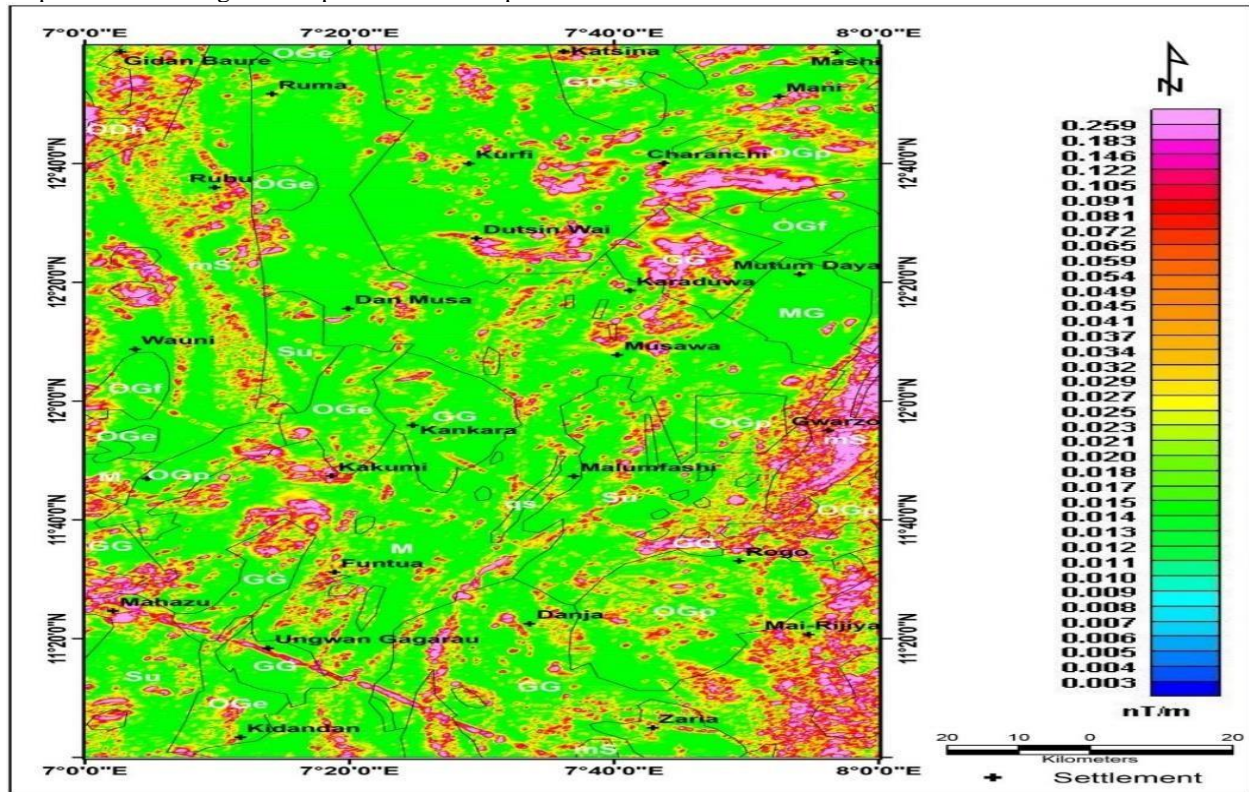


Figure 7: The analytic signal map of the area with geology

The First Vertical Derivative (FVD) map (Figure 8) Second Vertical Derivative (SVD) map (Figure 9) further enhances high-frequency, shallow structural features, clearly delineating lineaments in Mai-Jiriyia, Gwarzo, Charanchi, and along the NW-SE dyke-like feature. The

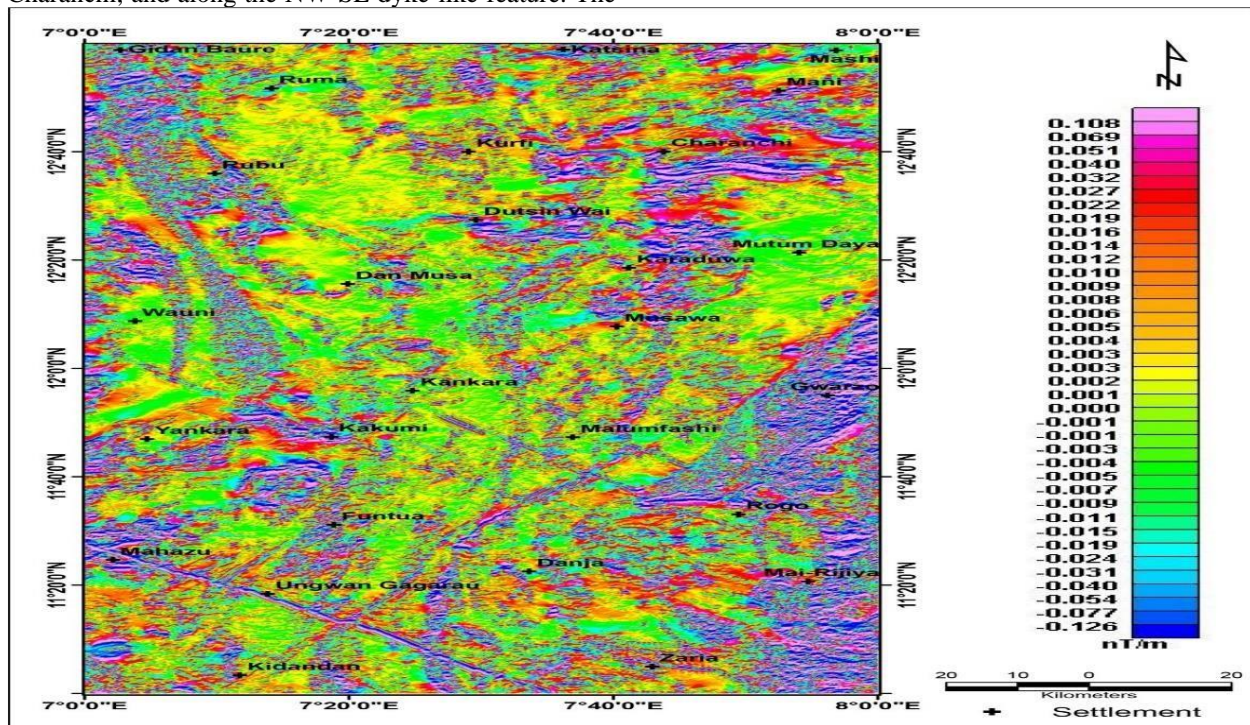


Figure 8: First vertical Derivative map

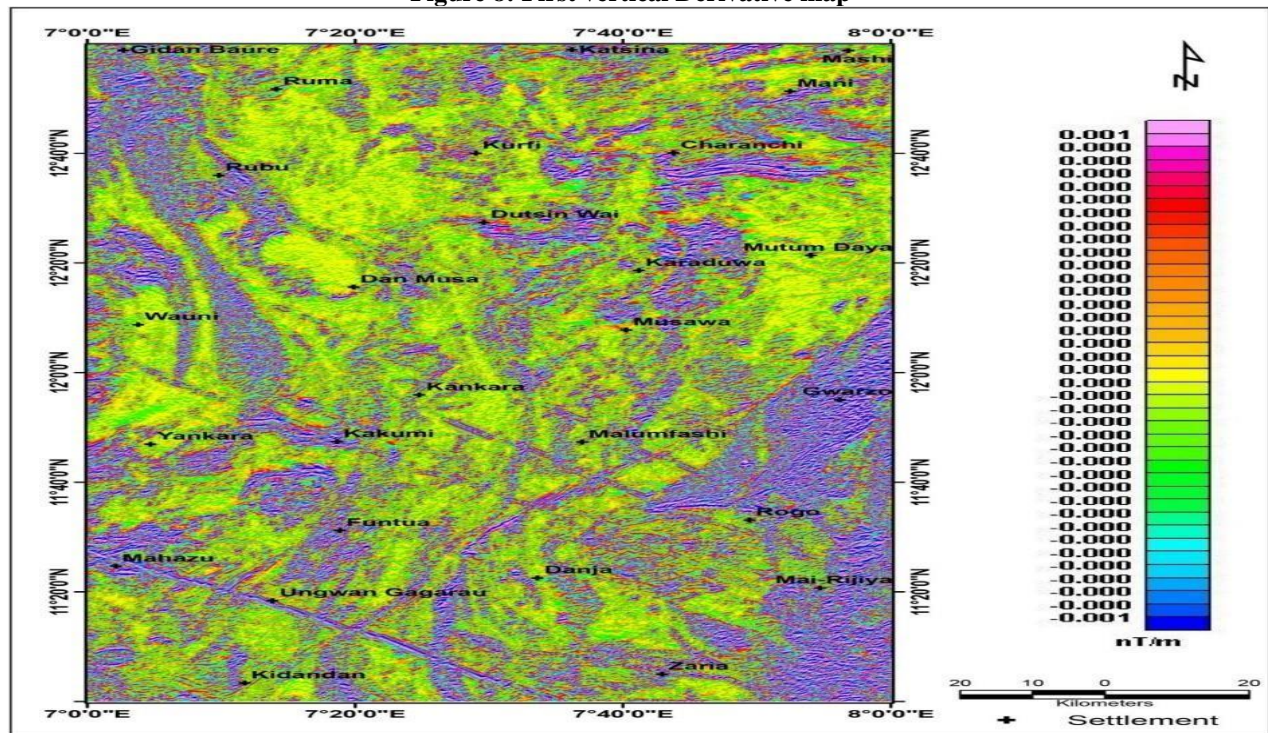


Figure 9: Second vertical Derivative map of the area

The Horizontal Gradient Magnitude (HGM) map (Figure 10) effectively delineates magnetic contacts and lineaments with reduced noise, particularly highlighting

the NW-SE dyke-like feature and contacts in the southeastern and northwestern zones.

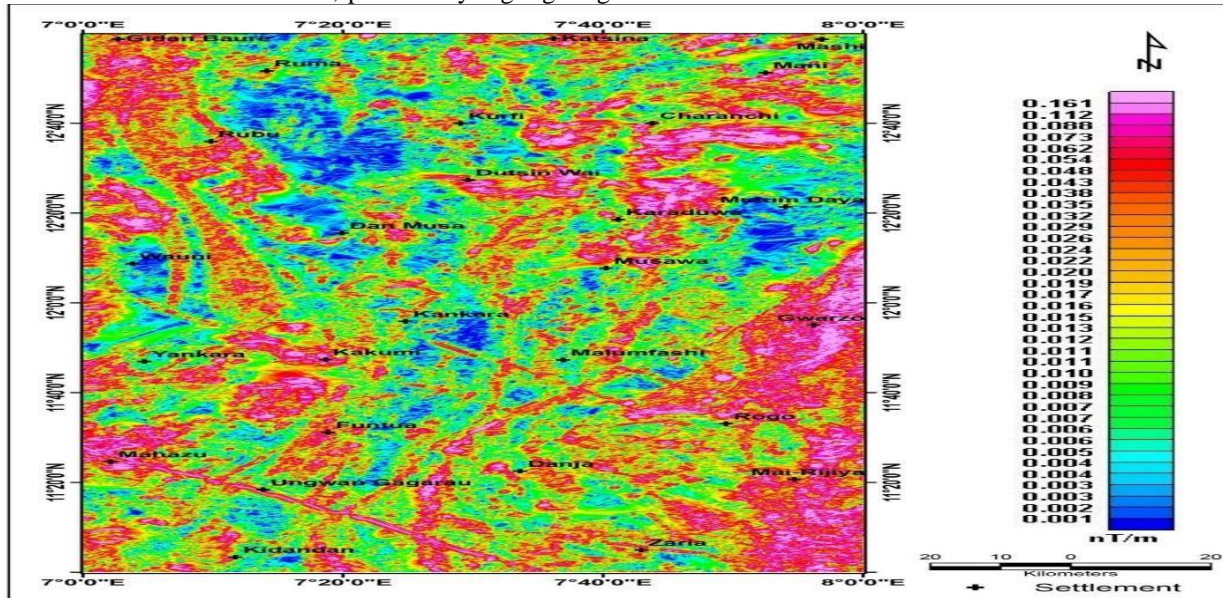


Figure 10: Horizontal gradient magnitude map of the study area

Structural maps were generated using the CET plug-in on AS, FVD, HGM, and RTE data. The AS-based structural map (Figure 11) shows concentration of lineaments in high AS zones with a dominant NE-SW trend. The FVD structural map (Figure 12) and HGM structural map (Figure 13) both highlight dense lineaments trending mainly WNW-ESE and NE-SW. The CET structural map derived from RTE data (Figure 14) reveals the highest

structural density, with dominant WNW-ESE trends, followed by NE-SW and subordinate NW-SE orientations. Rose diagrams accompanying these maps confirm the orientation trends.

AS Structures: Delineated using the CET plug-in, structures concentrate in high AS zones, with a dominant NE-SW trend (Figure 11).

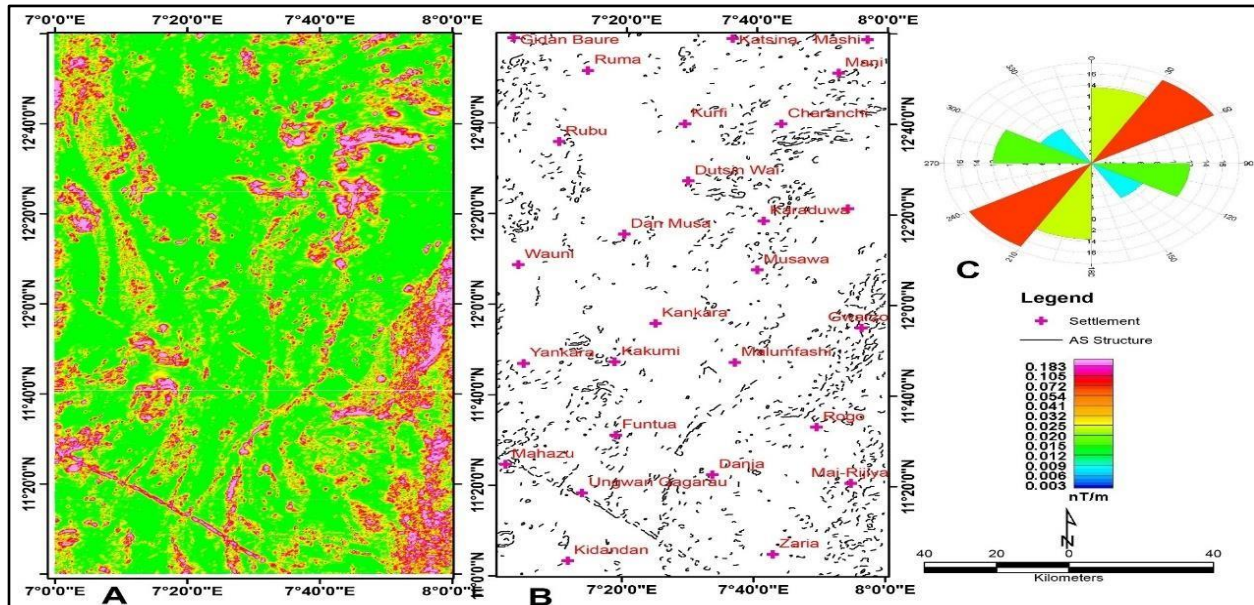


Figure 11: a. AS map, b. AS structure and c. Rose

FVD and HGM Structures: Both methods highlight shallow structures in WNW-ESE and NESW directions (Figures 12 and 13).

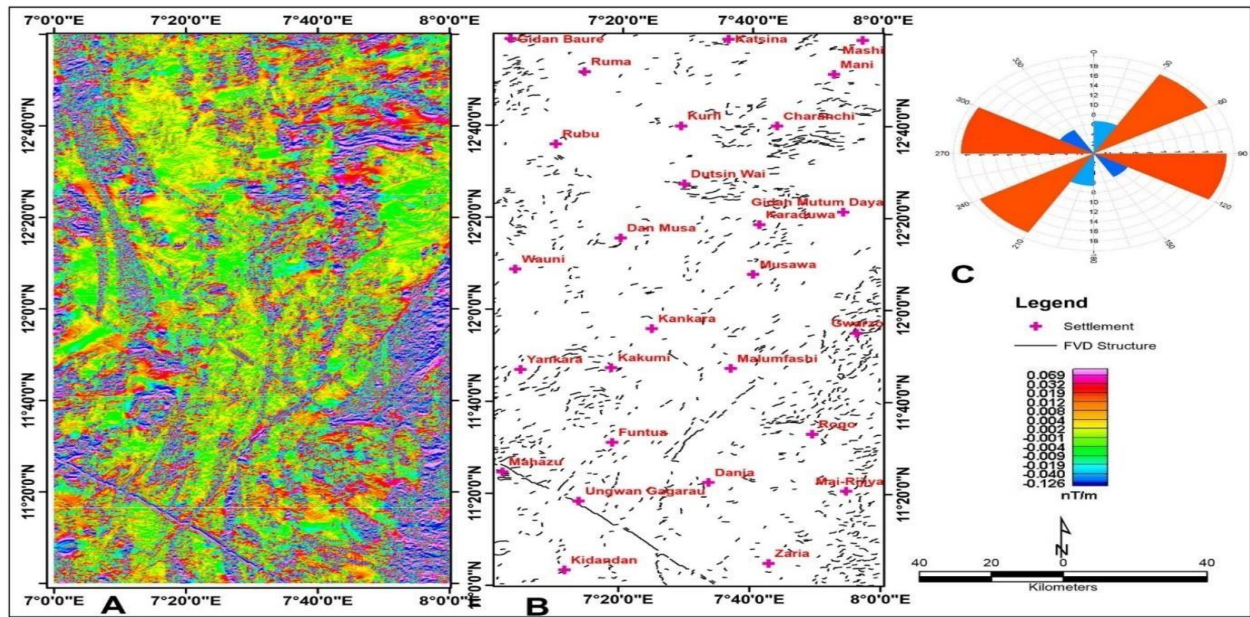


Figure 12: a. FVD map b. FVD structural map and c. Rose

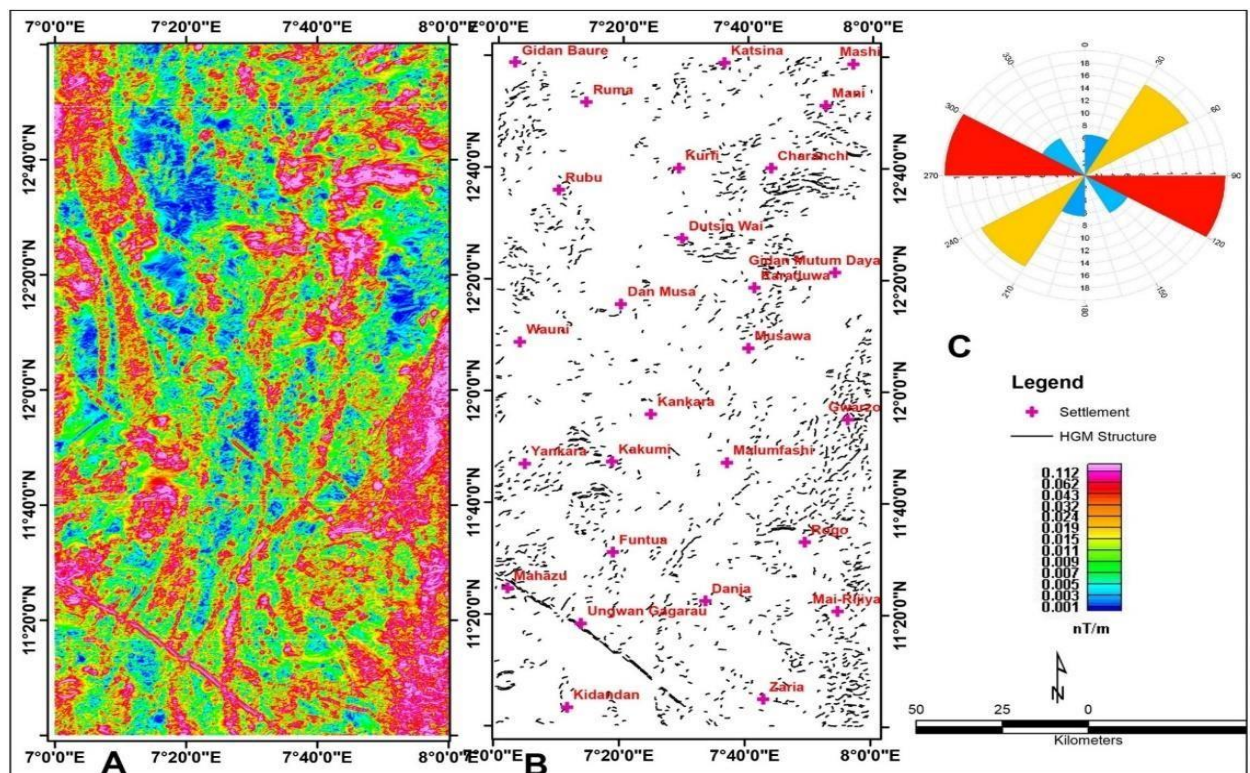


Figure 13: a. HGM map b. HGM structures and c. Rose diagram from CET Structures: Show higher structural density, predominantly WNW-ESE, followed by NESW and NW-SE (Figure 14).

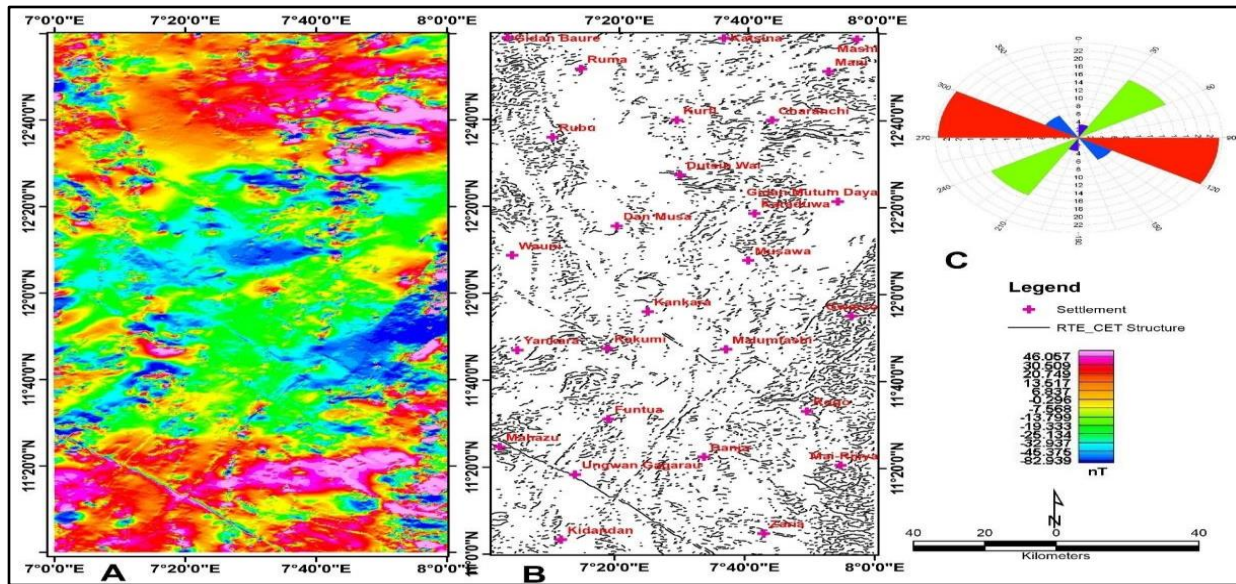


Figure 14: RTE map b. CET structures

High AS amplitude zones (0.091–0.259 nT/m) show strong spatial correlation with areas of high structural density. Figure 15 presents the SVD map with overlaid structures, the AS map with structures, and the structural density map, revealing that zones of elevated structural complexity coincide with high AS amplitudes, particularly in the southeast and northwest.

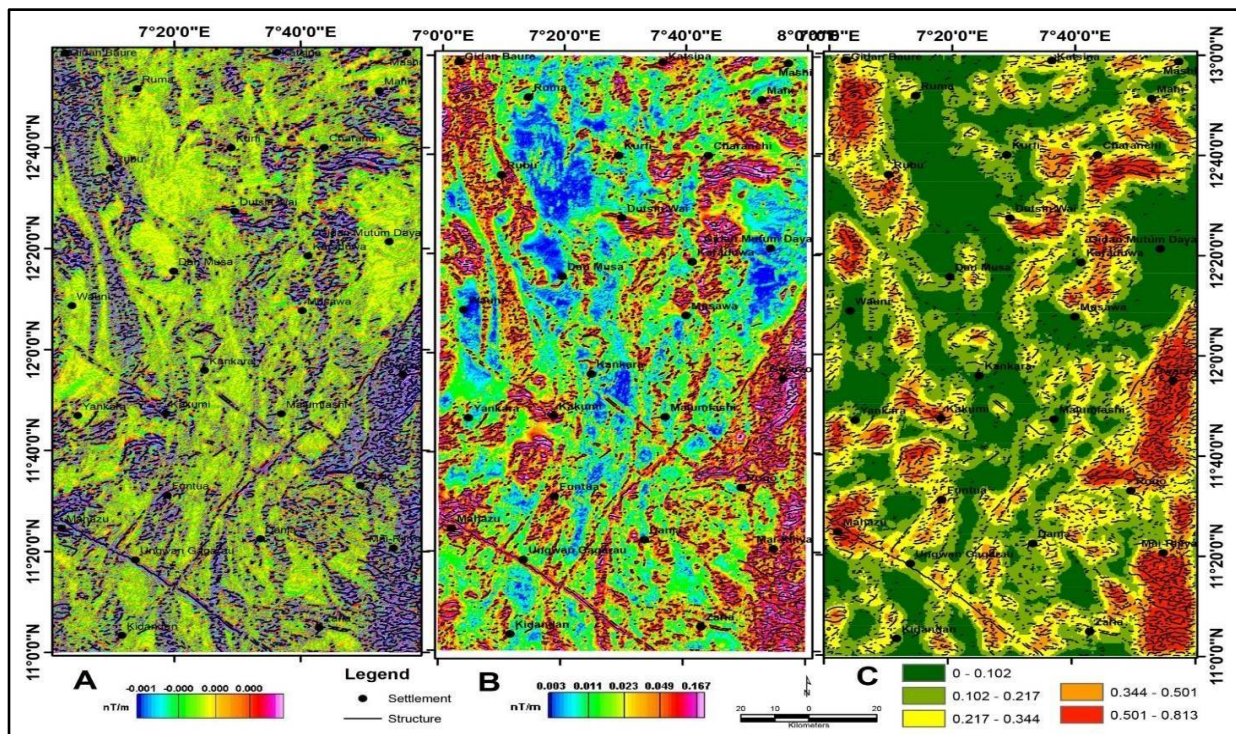


Figure 15: a. SVD map with structures b. AS map with structures and c. Structural density

Potential mineralisation zones were identified by overlaying high AS amplitude zones and high structural density areas with the geology of the study area. These prospective zones are concentrated in the southeastern (Mai-Jiriya, Gwarzo) and northwestern (Charanchi, Mani) regions, and along the prominent NW-SE dyke-

like feature through Mahazu and Ungwan Gagarau. Figure 16 shows the mineralisation zones overlaid on the geology, indicating strong association with

pelitic/muscovite schist and porphyritic granite lithologies.

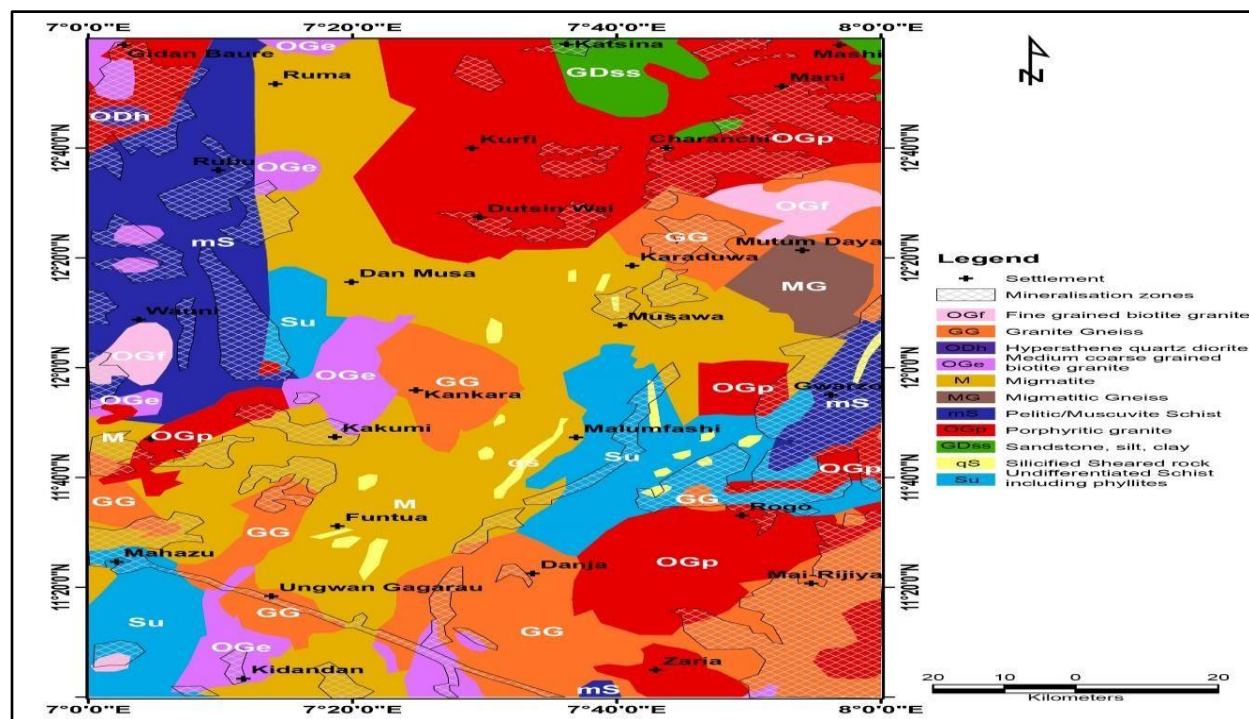


Figure 16: Mineralisation zones overlaid with the geology of the area

The TMI map when overlaid with the geological map (Figure 4) clearly highlighted lithological contrasts, with high magnetic anomalies associated with ferromagnetic-rich rocks such as porphyritic granite and hypersthene quartz diorite. The RMI (Figure 5) and RTE (Figure 6) maps successfully isolated and centered local anomalies, improving structural visibility at low magnetic latitudes. The Analytic Signal map (Figures 7) proved highly effective in delineating both high and low magnetic zones while being largely independent of magnetization direction. High AS amplitudes clearly highlighted shallow magnetic sources and the NW-SE dyke-like feature. The FVD (Figure 8) and SVD (Figure 9) enhanced shallow, high-frequency features and sharpened lineament boundaries, while the HGM (Figure 10) provided superior detection of magnetic contacts with minimal noise interference. Collectively, these edge-detection techniques complemented one another in mapping lineaments across the study area. The CET plugin successfully automated the extraction of complex structural patterns from different enhanced maps. Structures derived from AS data (Figure 11), FVD data (Figure 12), and HGM data (Figure 13) showed consistent lineament concentrations in zones of high magnetic gradients. The RTE-based CET analysis (Figure 14)

produced the most detailed structural map, revealing the highest lineament density. Rose diagrams across all methods confirmed dominant WNW-ESE and NE-SW trends, with a subordinate NW-SE orientation, consistent with Pan-African tectonic fabrics. A strong positive correlation exists between high AS amplitudes (0.091–0.259 nT/m) and zones of high structural density (Figure 15). Areas with elevated structural complexity, particularly in the southeast (Mai-Jiriya, Gwarzo) and northwest (Charanchi, Mani), coincide with high AS responses. This correlation suggests that intense deformation and fracturing enhanced the magnetic signature through increased magnetite concentration or shallow intrusive bodies. Potential mineralisation zones were successfully identified by integrating high AS amplitudes, high structural density, and geological data (Figure 16). The most prospective areas occur in the southeastern (Mai-Jiriya, Gwarzo) and northwestern (Charanchi, Mani) regions, as well as along the prominent NW-SE trending dyke-like feature through Mahazu and Ungwan Gagarau. These zones are predominantly hosted within pelitic/muscovite schist and porphyritic granite, indicating strong structural and lithological control on mineralisation. The NW-SE dyke-like structure is interpreted as a major mineralised corridor, likely acting

as a conduit for hydrothermal fluids. The multi-technique approach adopted in this study has demonstrated that zones characterised by high AS amplitudes and high structural density represent favourable targets for mineral exploration in the Malumfashi Schist Belt. These findings align with the structural control model of mineralisation commonly observed in northwestern Nigerian schist belts

CONCLUSION

Aeromagnetic data analysis revealed significant structural and mineralisation potential in Katsina State, with high magnetic anomalies and structural density zones in the southeast (Mai-Jiriya, Gwarzo) and northwest (Charanchi, Mani). The NW-SE dyke-like feature is a priority for exploration due to its consistent high AS and structural signatures.

Declaration of competing interest

The authors declare no known competing financial interest or personal relationships that might have affected the research presented in this paper.

REFERENCE

Abraham-Emmanuel, E. M., Tenda, A. M., and Aminu, M. D. (2021). A spatial reconnaissance survey for gold exploration in a schist belt. *Heliyon*, 6(11), e05564. <https://doi.org/10.1016/j.heliyon.2020.e05564>

Airo, M. L. (2007). Aeromagnetic signatures in gold exploration. *Exploration Geophysics*, 38(2), 123–130. <https://doi.org/10.1071/EG07014>

Ajibade, A. C., Woakes, M., and Rahaman, M. A. (1987). Proterozoic geology of Nigeria. *Geological Survey of Nigeria*.

Ajibade, A. C., Woakes, M., and Rahaman, M. A. (1988). The geology of the Malumfashi Schist Belt, northwestern Nigeria. *Journal of African Earth Sciences*, 7(5–6), 763–774. [https://doi.org/10.1016/0899-5362\(88\)90017-4](https://doi.org/10.1016/0899-5362(88)90017-4)

Andongma, W. T., Gajere, J. N., Amuda, A. K., Edmond, R. R. D., Faisal, M. and Yusuf, Y. D. (2021). Mapping of hydrothermal alterations related to gold mineralization within parts of the Malumfashi Schist Belt, North-Western Nigeria. *The Egyptian Journal of Remote Sensing and Space Science*, 24(3), 401–417. <https://doi.org/10.1016/j.ejrs.2020.12.004>

Ansari, A., and Alamdar, K. (2009). Analytic signal for depth estimation from magnetic anomalies. *Geophysics*, 74(3), L35–L40. <https://doi.org/10.1190/1.3106760>

Ekwok, S. E., Akpan, A. E., Achadu, O. I. M. and Eze, O. E. (2021). Structural and lithological interpretation of aero-geophysical data in parts of the Lower Benue

Trough and Obudu Plateau, southeast Nigeria. *Advances in Space Research*, 68(10), 3785–3800. <https://doi.org/10.1016/j.asr.2021.06.012>

Elawadi, E. A., Salem, A., and Ushijima, K. (2004). Detection of subsurface structures using magnetic and electrical methods in southwestern Egypt. *Geophysics*, 69(4), 1013–1022. <https://doi.org/10.1190/1.1776639>

Ferré, E. C., Caby, R., Peucat, J. J., Boesse, J. M., and Rahaman, M. A. (1998). Pan-African, postcollisional magmatism in the Nigeria-Benin-Niger Shield. *Tectonophysics*, 294(3–4), 277–294. [https://doi.org/10.1016/S0040-1951\(98\)00106-0](https://doi.org/10.1016/S0040-1951(98)00106-0)

Fitches, W. R., Ajibade, A. C., Egbuniwe, I. G., Holt, R. W., and Wright, J. B. (1985). Schist belts and mineral deposits in Nigeria. *Journal of African Earth Sciences*, 3(1), 23–30. [https://doi.org/10.1016/0899-5362\(85\)90020-8](https://doi.org/10.1016/0899-5362(85)90020-8)

Ge, J., Li, X., and Zhang, H. (2020). Advances in aeromagnetic survey techniques for mineral exploration. *Geophysical Journal International*, 222(3), 1456–1468. <https://doi.org/10.1093/gji/ggaa234>

Grant, F. S. (1985). Aeromagnetism, geology and ore environments, I. Magnetite in igneous, sedimentary and metamorphic rocks: An overview. *Geoexploration*, 23(3), 303–333. [https://doi.org/10.1016/0016-7142\(85\)90001-8](https://doi.org/10.1016/0016-7142(85)90001-8)

Ibrahim, A. A. (2003). Geology of the Nigerian Basement Complex. *Journal of Mining and Geology*, 39(2), 87–94.

Kearey, P., Brooks, M., and Hill, I. (2002). *An introduction to geophysical exploration* (3rd ed.). Blackwell Science.

Kogbe, C. A. (1976). The Cretaceous and Paleogene sediments of southern Nigeria. *Geological Survey of Nigeria Bulletin*, 32, 1–25.

Lawal, T. O., Ogah, A. J., Abubakar, A. (2024). Solid mineral potential evaluation using integrated aeromagnetic and aeroradiometric datasets. *Scientific Reports*, 14, 1637. <https://doi.org/10.1038/s41598024-52270-6>

Macleod, I. N., Jones, K., and Dai, T. F. (1993). 3-D analytic signal in the interpretation of total magnetic field data at low magnetic latitudes. *Exploration Geophysics*, 24(4), 679–688. <https://doi.org/10.1071/EG993679>

Murthy, K. S. R. (2007). *Geophysical exploration for mineral deposits*. Indian Geophysical Union.

- Nigerian Geological Survey Agency. (2006). *Geological map of Nigeria*. Nigerian Geological Survey Agency. Geophysics, 35(2), 293–302. <https://doi.org/10.1190/1.1440092>
- Nzekwu, B. A., and Abraham-Emmanuel, E. M. (2022). Evolution of the Nigerian Basement Complex: Current Status and Suggestions for Future Research. *Journal of Mining and Geology*, 58(1), 1–15. Tawey, M. D., Sanusi, Y. A., and Salako, K. A. (2023). Structural mapping using the CET plug-in for aeromagnetic data analysis. *Geophysical Prospecting*, 71(3), 234–245. <https://doi.org/10.1111/1365-2478.13210>
- Olasunkanmi, N. K., Adebayo, O. S., and Salako, K. A. (2020). Aeromagnetic data interpretation for mineral exploration in Nigeria. *Journal of Mining and Geology*, 56(1), 23–34. Tawey, M. D., Sanusi, Y. A. and Salako, K. A. (2024). Application of CET Grid Analysis and Edge Detection Technique on Aeromagnetic Data for Structural Mapping in Parts of North-Central Nigeria. *Journal of Basic and Applied Science Research*, 14(3), 1-12.
- Onyewuchi, R. A., Lawal, K. M., and Afolabi, O. A. (2012). Lineament extraction from aeromagnetic data over part of southern Nigeria. *Journal of Mining and Geology*, 48(1), 45–53. Telford, W. M., Geldart, L. P., and Sheriff, R. E. (1990). *Applied geophysics* (2nd ed.). Cambridge University Press.
- Oyeniyi, T. O., Falade, A. H., and Adepelumi, A. A. (2022). Aeromagnetic Reconnaissance of Zagami Meteorite Impact Site, Katsina State, North-Western Nigeria for an Impact Crater. *International Journal of Engineering Research and Technology*, 11(4), 1–10. Usman, A. O., Nomeh, J. S. and Abraham, E. M. (2025). Subsurface structural mapping a tool in understanding the Geodynamics of Mineralization within the North-Central Precambrian Basement of Nigeria, using aeromagnetic dataset. *Earth Science Informatics*, 18, 169. <https://doi.org/10.1007/s12145-024-01492-3>
- Phillips, J. D. (2000). Locating magnetic contacts using the horizontal gradient magnitude. *SEG Annual Meeting Abstracts*, 70, 123–128. <https://doi.org/10.1190/1.1816253>
- Reynolds, J. M. (2011). *An introduction to applied and environmental geophysics* (2nd ed.). Wiley-Blackwell. Usman, A. O., Nomeh, J. S., Abraham, E. M. and Azuoko, G.-B. (2025). Uncovering the hidden mineral treasure of the Jurassic Younger Granite region of Nigeria using integrated magnetic geophysical techniques. *Frontiers in Earth Science*, 13, 1568232. <https://doi.org/10.3389/feart.2025.1568232>
- Salawu, N. B., Omosanya, K. O. L., Eluwole, A. B., Ajadi, J., and Adebisi, L. S. (2023). Structurally-controlled Gold Mineralization in the Southern Zuru Schist Belt NW Nigeria: Application of Remote Sensing and Geophysical Methods. *Journal of Applied Geophysics*, 211, Article 104969. <https://doi.org/10.1016/j.jappgeo.2023.104969>
- Spector, A., Grant, F. S. and Parker, P. B. (1970). Statistical models for interpreting aeromagnetic data. Zlotnikov, M. (2012). Geophysical methods for mineral exploration: A review. *Journal of Geophysical Research*, 117(B8), B08205. <https://doi.org/10.1029/2012JB009123>